

Translocator Protein PET Imaging for Glial Activation in Multiple Sclerosis

Unsong Oh · Masahiro Fujita · Vasiliki N. Ikonomidou · Iordanis E. Evangelou · Eiji Matsuura · Erin Harberts · Joan Ohayon · Victor W. Pike · Yi Zhang · Sami S. Zoghbi · Robert B. Innis · Steven Jacobson

Received: 22 July 2010 / Accepted: 30 August 2010 / Published online: 25 September 2010
© US Government 2010

Abstract Glial activation in the setting of central nervous system inflammation is a key feature of the multiple sclerosis (MS) pathology. Monitoring glial activation in subjects with MS, therefore, has the potential to be informative with respect to disease activity. The translocator protein 18 kDa (TSPO) is a promising biomarker of glial activation that can be imaged by positron emission tomography (PET). To characterize the in vivo TSPO expression in MS, we analyzed brain PET scans in subjects with MS and healthy volunteers in an observational study using [¹¹C]PBR28, a newly developed translocator protein-specific radioligand. The [¹¹C]PBR28 PET showed altered compartmental distribution of TSPO in the MS brain compared to healthy volunteers ($p=0.019$). Focal increases in [¹¹C]PBR28 bind-

ing corresponded to areas of active inflammation as evidenced by significantly greater binding in regions of gadolinium contrast enhancement compared to contralateral normal-appearing white matter ($p=0.0039$). Furthermore, increase in [¹¹C]PBR28 binding preceded the appearance of contrast enhancement on magnetic resonance imaging in some lesions, suggesting a role for early glial activation in MS lesion formation. Global [¹¹C]PBR28 binding showed correlation with disease duration ($p=0.041$), but not with measures of clinical disability. These results further define TSPO as an informative marker of glial activation in MS.

Keywords Multiple sclerosis · Translocator protein · PET · Glial activation

Unsong Oh and Masahiro Fujita contributed equally to the manuscript.

U. Oh · I. E. Evangelou · E. Harberts · J. Ohayon · S. Jacobson (✉)
Neuroimmunology Branch, National Institute of Neurological Disorders and Stroke, National Institutes of Health,
10 Center Drive, Bldg 10 Rm 5C103,
Bethesda, MD 20892, USA
e-mail: jacobsons@ninds.nih.gov

M. Fujita · V. W. Pike · Y. Zhang · S. S. Zoghbi · R. B. Innis
Molecular Imaging Branch, National Institute of Mental Health,
National Institutes of Health,
Bethesda, MD, USA

V. N. Ikonomidou
Department of Electrical and Computer Engineering,
The Volgenau School of Information Technology
and Engineering, George Mason University,
Fairfax, VA, USA

E. Matsuura
Department of Neurology and Geriatrics, Kagoshima University
Graduate School of Medical and Dental Sciences,
Kagoshima, Japan

Introduction

Glial activation in the setting of central nervous system (CNS) inflammatory demyelination is the pathologic hallmark of multiple sclerosis (MS). Activated microglia and reactive astrocytes not only augment CNS inflammation but may contribute to mechanisms of neurodegeneration such as glutamate excitotoxicity (Werner et al. 2001) and oxidative stress (Bagasra et al. 1995). Therefore, monitoring glial activation in subjects with MS has the potential to be an informative measure of disease activity.

Translocator protein 18 kDa (TSPO), formerly termed the peripheral benzodiazepine receptor, has been imaged by positron emission tomography (PET) as a marker of glial activation. TSPO is an outer mitochondrial membrane protein involved in the control of steroidogenesis (McEneaney et al. 1992). During CNS inflammation, TSPO expression is increased in activated microglia, infiltrating macrophages and reactive astrocytes (Cosenza-Nashat et al.

2008). The TSPO-selective radioligand [^{11}C](R)-PK11195 has been studied in several neurologic disorders including MS. [^{11}C]PK11195 showed promise as a biomarker in MS, showing increased TSPO expression in areas of focal MS pathology defined by magnetic resonance imaging (MRI; Banati et al. 2000). Newer TSPO-selective radioligands such as the aryloxyanilide-based [^{11}C]PBR28 has the potential to improve on these findings based on its higher brain uptake and specific binding (Kreisl et al. 2010).

In this paper, we report the study of TSPO expression in subjects with MS by PET using the new selective radioligand [^{11}C]PBR28. To characterize the TSPO expression in MS, we compared the global and compartmental [^{11}C]PBR28 binding in subjects with MS to that of healthy donors. Regions of interest analysis was performed to evaluate [^{11}C]PBR28 binding in MRI-defined MS lesions compared to normal-appearing white matter (NAWM). Correlations between [^{11}C]PBR28 binding levels and clinical parameters were also examined to provide preliminary evidence regarding TSPO expression as a biomarker in MS.

Materials and methods

Subjects

All subjects provided informed written consent under a National Institutes of Health Clinical Center Institutional

Review Board-approved research protocol. Subjects with definite diagnosis of MS (McDonald et al. 2001) meeting inclusion criteria, and age, gender-matched healthy volunteers were consecutively enrolled. Subject demographics are provided in Table 1. Eleven subjects with MS and seven healthy volunteers underwent brain [^{11}C]PBR28 PET and brain MRI scanning as detailed below. A 4-month follow-up brain [^{11}C]PBR28 PET was obtained in a subset (six) of the subjects with MS.

Radioligand

[^{11}C]PBR28 was produced in >99% radiochemical purity by ^{11}C -methylation of its *O*-desmethyl precursor, as originally described (Briard et al. 2008).

PET imaging with arterial blood sampling

The high-resolution research tomograph (HRRT; Siemens/CPS, Knoxville, TN, USA) camera was used. The HRRT camera has a reconstructed resolution of 2.5 mm full-width half-maximum in all directions in 3-D mode. After injection of 650 ± 92 MBq (specific activity at time of injection of 170 ± 81 GBq/ μmol) of [^{11}C]PBR28, PET scans were acquired for 120 to 150 min in 33 to 39 frames with scan duration ranging from 30 s to 5 min. As described previously, metabolite-corrected arterial input function was measured by blood sampling followed by radio-HPLC, and

Table 1 Subject characteristics

Subject	Diagnosis	Age	Sex	Disease duration (years)	EDSS	MSFC (Z-score)	Disease-modifying drugs	Gd+ MRI
MS 1	MS	45	F	0.5	2.0	0.544	None	Yes
MS 2	MS	36	M	5	1.5	1.005	Interferon beta	Yes
MS 3	MS	39	F	15	1.5	0.480	Interferon beta	No
MS 4	MS	34	F	3	4.0	-0.366	Natalizumab	No
MS 5	MS	67	M	10	2.5	0.598	None	Yes
MS 6	MS	61	M	27	2.0	0.671	Glatiramer acetate	No
MS 7	MS	55	F	18	1.5	0.347	Interferon beta	No
MS 8	MS	57	F	36	6.0	-0.959	None	No
MS 9	MS	40	F	2	1.0	0.879	Glatiramer acetate	No
MS 10	MS	54	M	22	6.5	-1.327	Interferon beta	No
MS11	MS	59	F	15	6.0	-0.072	Interferon beta	No
HV 1	HV	40	M					
HV 2	HV	37	M					
HV 3	HV	43	F					
HV 4	HV	35	F					
HV 5	HV	40	F					
HV 6	HV	62	M					
HV 7	HV	57	M					

MS multiple sclerosis, HV healthy volunteer, EDSS expanded disability status scale, MSFC multiple sclerosis functional composite score, Gd+ MRI the presence of gadolinium contrast-enhancing lesions on brain MRI at the time of PET

plasma free fraction (f_p) of [^{11}C]PBR28 was also measured (Fujita et al. 2008). Approximately 10% of the subjects studied to date show low-affinity binding of [^{11}C]PBR28 to TSPO in brain and periphery. Low affinity binders to [^{11}C]PBR28 were excluded following the criteria of Kreisl and colleagues (Kreisl et al. 2010).

PET processing

[^{11}C]PBR28 binding was measured in each voxel by calculating total distribution volume, V_T using the Logan plot (Logan et al. 1990) and metabolite-corrected arterial input function based on 2-h brain and blood data. V_T is brain activity normalized to plasma total (free plus protein-bound) [^{11}C]PBR28 levels and corresponds to total (specific plus nondisplaceable) binding. Our previous study showed that 90-min data acquisition was adequate to measure [^{11}C]PBR28 binding accurately (Fujita et al. 2008). To be conservative, we used 2-h data for the analysis of all scans in the current study. For noisy data such as those in each voxel, the Logan plot is known to show smaller V_T than compartmental models. Compartmental modeling is believed to be more resistant to errors caused by noise (Logan 2003). We calculated V_T in each voxel to allow inspection of V_T values in all brain areas including those with and without changes in MRI by comparing the co-registered images. In gadolinium contrast-enhancing lesions, the Logan plot using voxel data showed only 9% smaller V_T values than that based on region-of-interest data, and was therefore used as the primary method of PET analysis. To take into account inter-subject and between-scan variability in f_p , V_T was normalized to f_p , and V_T/f_p was used as a measure of total binding of [^{11}C]PBR28. All PET processing was performed in PMOD software (PMOD Technologies Ltd., Zurich, Switzerland)

MRI acquisition

Subjects underwent a screening 1.5 T brain MRI. The exam included 2D T_1 -weighted spin echo; dual-echo fast spin-echo sequence providing both proton density and T_2 -weighted images; a T_2 -weighted fluid-attenuated inversion recovery (FLAIR) sequence; and three acquisitions of a 3-D inversion recovery prepared fast spoiled gradient echo (IR-FSPGR) sequence. In MS subjects, a second T_1 -weighted spin echo was performed after administration of a single-dose gadolinium gadopentate (Magnevist, Berlex Laboratories). All 2-D MRIs had 3 mm slice thickness whereas the 3-D IR-FSPGR had 1.2 mm slice thickness. Brain MRI was repeated for subjects with MS at the time of the PET scan (± 7 days). Additional brain MRI covering the periods both before

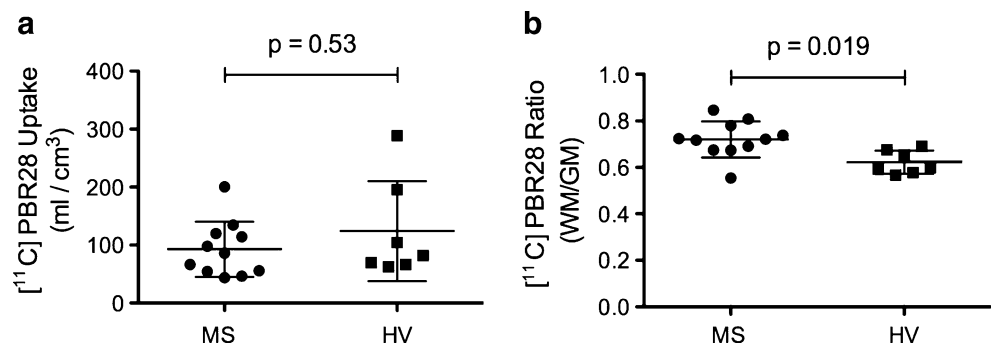
and after the PET scan was available for a number of subjects enrolled in longitudinal follow-up.

MRI processing

T_1 lesions were marked on the pre-contrast T_1 -weighted spin-echo images by an investigator blinded to the PET imaging; a lesion was marked as such if it was hypointense on the T_1 -weighted images and hyperintense on the T_2 -weighted images. T_2 lesions were marked on the T_2 FLAIR images. Contrast-enhancing lesions were marked on the post-contrast T_1 -weighted spin-echo images. All lesion markings were done manually using Medical Image Processing, Analysis and Visualization. In addition, for each contrast-enhancing lesion, we created a mask of contralateral normal-appearing white matter. Subsequently, all images and masks were registered to the PET scan using an affine transform with 6° of freedom, as implemented in Medical Imaging NetCDF tools. The three acquisitions of the 3-D IR-FSPGR sequence were registered and averaged in order to increase signal-to-noise ratio. Subsequently, they were segmented into gray matter, white matter, and cerebrospinal fluid using FAST (Zhang et al. 2001). Segmented tissue masks were corrected for lesions. Subcortical structures were then segmented and individual masks for the thalamus, caudate, putamen, pallidum, nucleus accumbens, amygdala, and hippocampus were generated using FMRIB's Integrated Registration and Segmentation Tool. These masks were then used to further correct the gray and white matter masks. The resulting masks were registered to the PET image space using an affine transform with 6° of freedom, and were then used to calculate average [^{11}C]PBR28 binding values in lesions, white, and gray matter. The corrected masks were also used to calculate brain parenchymal and gray matter fraction as atrophy measures. Since direct comparison of absolute brain parenchymal volume between the patients and healthy control subjects may be obscured by differences in head size, particularly across sex and age, we normalized head size variability by using fractional gray matter volume and fractional white matter volume, which were computed as percentages of the intracranial volume; fractional gray matter = gray matter / (gray matter + white matter + CSF).

[^{11}C]PBR28 binding levels were compared between contrast-enhancing lesions and the contralateral NAWM by drawing the same size of region of interest on the parametric images where V_T/f_p values were calculated in each voxel using the Logan plot (i.e., V_T/f_p maps). [^{11}C]PBR28 binding at periplaque white matter was assessed visually after multiplying the V_T/f_p maps with the segmented white matter mask and thresholding it to the level of average gray matter [^{11}C]PBR28 binding. The threshold

Fig. 1 Global and compartmental [^{11}C]PBR28 binding in subjects with MS compared to healthy volunteers. **a** Mean (\pm SD) brain parenchymal [^{11}C]PBR28 binding in subjects with multiple sclerosis (MS) compared to healthy volunteers (HV). **b** The ratios of white matter to gray matter fraction [^{11}C]PBR28 binding (WM/GM) in subjects with MS compared to HV



provided normalization based on each individual patient's binding level similar to the one used by Versijpt and colleagues (Versijpt et al. 2005).

Where interval PET scans were available on the same subject, the resulting V_T/f_p maps were registered using an affine transformation, and difference maps were calculated to identify regions of increased and decreased PBR binding.

Statistical analysis

The Kolmogorov–Smirnov test was used as a test of normality. For comparison between groups, Mann–Whitney test was used. Paired comparisons were tested by Wilcoxon signed rank test. Pearson correlation coefficients were calculated to assess relationship between [^{11}C]PBR28 binding and clinical parameters. All statistical analysis was performed in Prism (GraphPad Software Inc.; La Jolla, CA).

Results

[^{11}C]PBR28 PET: MS vs. healthy volunteers

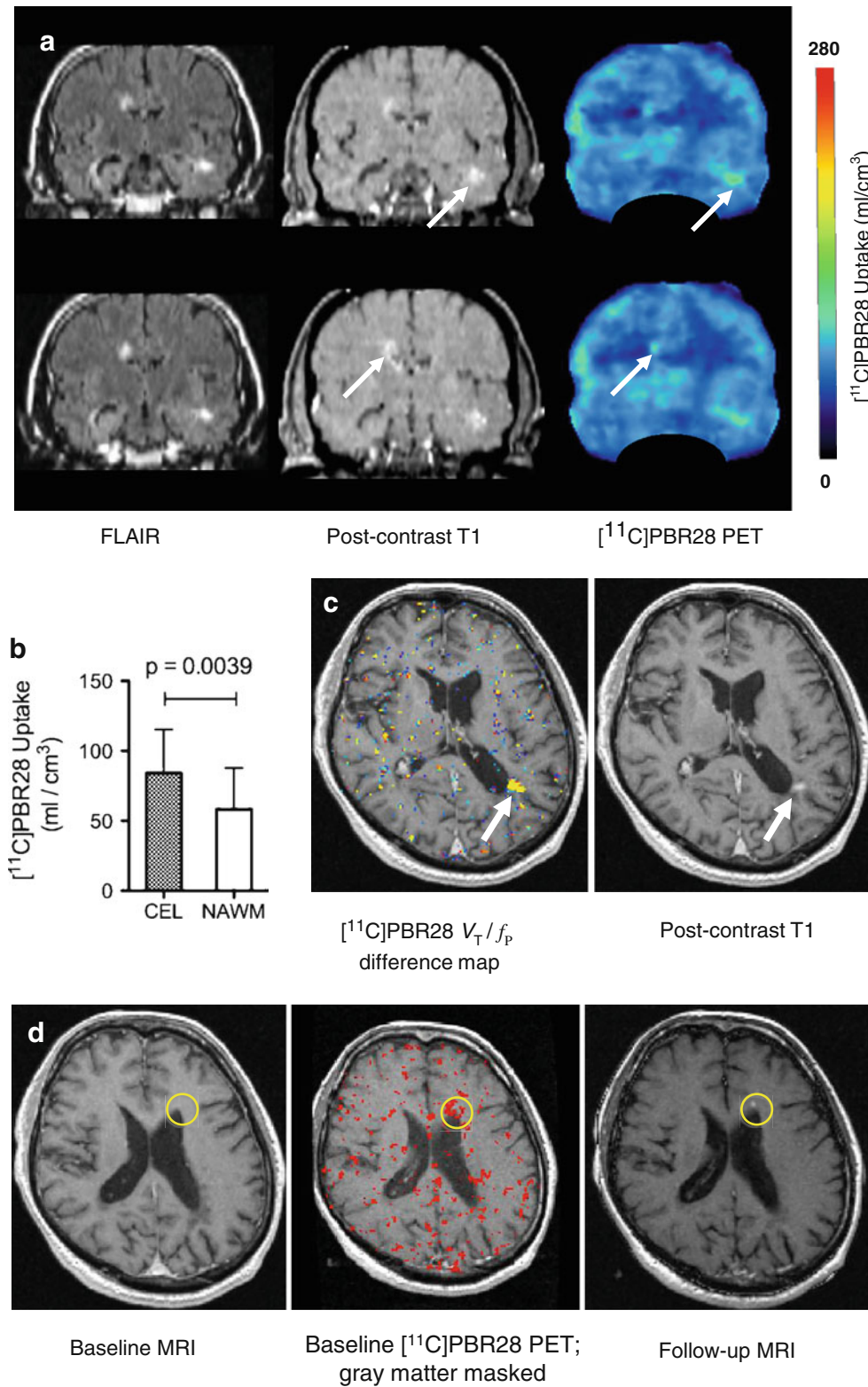
Subjects with MS and healthy volunteers were well matched for age (49.7 ± 11.3 vs. 44.9 ± 10.4). The clinical characteristics of subjects with MS are provided in Table 1. As shown in Fig. 1a, the mean (\pm SD) brain parenchymal [^{11}C]PBR28 binding for subjects with MS (102 ± 47 ml/cm³) did not differ significantly from that of healthy volunteers (124 ± 86 ml/cm³; $p=0.53$; Mann–Whitney). However, the ratio of white matter fraction [^{11}C]PBR28 binding to gray matter fraction [^{11}C]PBR28 binding was significantly higher in MS compared to healthy volunteers ($p=0.019$; Mann–Whitney; Fig. 1b), suggesting altered compartmental distribution of TSPO expression in the MS brain. Compared separately, the differences in neither the white matter fraction [^{11}C]PBR28 binding nor the gray matter fraction [^{11}C]PBR28 binding reached statistical significance between MS and healthy volunteers (data not shown). We found no significant correlation between mean

brain parenchymal [^{11}C]PBR28 binding and T₂-hyperintense lesion load, T₁-hypointense lesion load, or brain parenchymal fraction (data not shown).

Focal increase in TSPO expression corresponds to gadolinium contrast-enhancing lesions

To further characterize TSPO expression in MS, regions of interest analysis was performed to examine the relationship between [^{11}C]PBR28 binding and MRI-defined lesions including gadolinium contrast-enhancing lesions, T₂-hyperintense lesions and T₁-hypointense lesions. Gadolinium contrast-enhancing lesions were identified on brain MRI of MS subjects. A total of ten MRI contrast-enhancing lesions were present in three subjects at the time of the PET scan. Contralateral NAWM was identified for comparison. Figure 2a shows a representative contrast-enhancing lesion (arrow) on T₁-weighted and FLAIR MRI of an MS subject with the corresponding region on PET showing elevated [^{11}C]PBR28 binding. Contrast-enhancing lesions demonstrated significantly higher [^{11}C]PBR28 binding than contralateral NAWM ($p=0.0039$; Wilcoxon signed rank; Fig. 2b). The correspondence between increased [^{11}C]PBR28 binding and contrast enhancement was further demonstrated by comparing baseline and 4-month follow-up brain [^{11}C]PBR28 PET for an MS subject who demonstrated a new contrast-enhancing lesion on MRI at the 4-month follow-up. As shown in Fig. 2c, the region of highest interval increase in [^{11}C]PBR28 binding (arrow) corresponded to a newly contrast-enhancing lesion.

Increased focal [^{11}C]PBR28 binding preceded the development of some gadolinium-enhancing lesions. This was shown in two MS subjects that developed new gadolinium contrast-enhancing lesions on a follow-up MRI 1 month after the PET scan. In one MS subject (MS5), a region of focal increased [^{11}C]PBR28 binding in an area of NAWM at the time of the PET scan corresponded to a contrast-enhancing lesion at a follow-up MRI exam 1 month later (Fig. 2d). Similarly, in another subject (MS3), a region of increased [^{11}C]PBR28 binding corresponding to a non-enhancing T₁-hypointense lesion preceded the development of new



contrast enhancement of that lesion, seen on a 1-month follow-up MRI (data not shown). Although regions of increased [¹¹C]PBR28 binding were not exclusively predictive of the development of new MRI lesions, these results

suggest that the temporal dynamics of increased [¹¹C]PBR28 binding and contrast enhancement may differ, providing additional information regarding early lesion formation not provided by MRI alone.

Fig. 2 Gadolinium contrast-enhancing lesions show focal increase in [^{11}C]PBR28 binding. **a** Fluid-attenuated inversion recovery (FLAIR) and post-contrast T₁-weighted (post-contrast T₁) MRI, and [^{11}C]PBR28 PET from a subject with MS (MS3) showing increased [^{11}C]PBR28 binding in the areas corresponding to gadolinium-enhancing lesion (arrows). **b** [^{11}C]PBR28 binding in gadolinium contrast-enhancing lesions (CEL) compared to contralateral normal-appearing white matter (NAWM). Error bars indicate \pm SD. **c** MRI co-registered baseline-to-follow-up [^{11}C]PBR28 V_T difference map (left) and post-contrast T₁-weighted MRI (right) showing a region of interval increase in [^{11}C]PBR28 binding corresponding to a gadolinium contrast-enhancing lesion (arrows). **d** Post-contrast T₁-weighted MRI (left) and co-registered [^{11}C]PBR28 V_T difference map (center) with increased [^{11}C]PBR28 binding that precedes a gadolinium enhancement of the same region a month later (right)

There was less of a correspondence between [^{11}C]PBR28 binding and non-enhancing T₂-hyperintense and T₁-hypointense lesions. As a group, T₂-hyperintense lesions did not demonstrate increased [^{11}C]PBR28 binding (data not shown). Similarly, T₁-hypointense lesions did not show increased [^{11}C]PBR28 binding within the boundaries of the lesions. However, T₁-hypointense lesions were frequently associated with peri-lesional increased [^{11}C]PBR28 binding. Seventy one percent (70/98) of the non-enhancing T₁-hypointense lesions examined showed varying levels of [^{11}C]PBR28 peri-lesional binding above average gray matter binding level.

Increased TSPO expression in subjects with longer disease duration of MS

The relationships between [^{11}C]PBR28 PET and MS-relevant clinical parameters were examined. Age, disease duration, and neurological disability as measured by expanded disability status scale (EDSS) and the multiple sclerosis functional composite (MSFC) score were examined with respect to mean brain parenchymal [^{11}C]PBR28 binding in subjects with MS. There was a positive

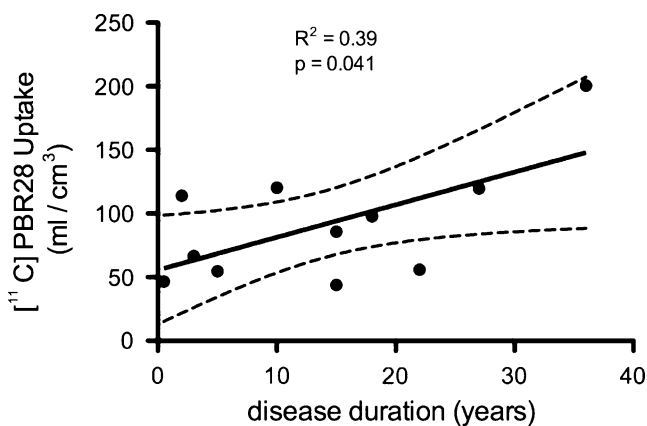


Fig. 3 Correlation between disease duration and mean brain parenchymal [^{11}C]PBR28 binding in subjects with MS ($R^2=0.39$, $p=0.041$)

correlation between the mean brain parenchymal [^{11}C]PBR28 binding and disease duration in subjects with MS ($r^2=0.39$, $p=0.041$; Pearson; Fig. 3), suggesting increased TSPO expression in subjects with longer duration of MS. No significant correlations were observed between brain parenchymal [^{11}C]PBR28 binding and age ($p=0.25$), EDSS ($p=0.89$), or the MSFC z-score ($p=0.68$).

Discussion

The results of the [^{11}C]PBR28 PET show altered compartmental distribution of TSPO expression in subjects with MS compared to healthy volunteers. The ratio of white matter fraction to gray matter fraction [^{11}C]PBR28 binding was significantly elevated in MS, suggesting a change in the relative distribution of TSPO even though the global [^{11}C]PBR28 binding was not significantly different between MS and healthy volunteers. This may be due to the fact that normalized parameters such as the ratio of white matter to gray matter fraction [^{11}C]PBR28 binding are less noisy and more sensitive for detecting differences between groups. The increase in the ratio of white matter to gray matter TSPO expression could indicate either a relative increase in the white matter TSPO or a relative decrease in the gray matter TSPO in MS. Neither region showed statistically significant differences in [^{11}C]PBR28 binding between MS and healthy volunteers when compared separately, thus, we could not conclusively attribute the increased ratio to changes in a single compartment.

Gadolinium contrast-enhancing lesions were associated with focal increases in [^{11}C]PBR28 binding. Areas corresponding to contrast-enhancing lesions were significantly higher with respect to [^{11}C]PBR28 binding than the contralateral NAWM, and the development of a new contrast-enhancing lesion on MRI was accompanied by interval increase in [^{11}C]PBR28 binding. The most likely source of increased TSPO expression in the contrast-enhancing lesions of MS brain is activated microglia and macrophage (Katz et al. 1993). The focal increase in TSPO expression detected by [^{11}C]PBR28 PET that corresponds to and precedes the appearance of gadolinium enhancement on MRI may support a role for early microglial activation in the formation of some MS lesions. Although regions of increased [^{11}C]PBR28 binding were not exclusively predictive of the development of new gadolinium-enhancing lesions, early glial activation in MS lesion formation is consistent with reports in the literature. Pathologic studies have shown evidence to suggest that microglial activation occurs very early in the formation of MS lesions, in some cases preceding lymphocytic infiltration and myelin loss (Henderson et al. 2009). Thus, differences in the temporal dynamics of contrast enhancement and the corresponding

increase in [^{11}C]PBR28 binding suggest that the [^{11}C]PBR28 PET offers additional information regarding focal CNS inflammation not captured by conventional gadolinium contrast-enhanced MRI.

We found a trend towards increased [^{11}C]PBR28 binding with increasing disease duration in MS. A correlation between [^{11}C]PBR28 binding and measures of clinical disability, however, was not detected, suggesting that changes in TSPO expression are not as closely linked to the accumulation of disability in MS. Although earlier studies maintained that TSPO expression is restricted to activated microglia/macrophage in MS (Banati et al. 2000), more recent studies have shown increased TSPO expression in reactive astrocytes as well. In particular, one study showed a temporal evolution in the cellular localization of TSPO in MS where TSPO expression was prominent in activated microglia/macrophage in active MS plaques, but was more prominent in reactive astrocytes in chronic MS plaques (Cosenza-Nashat et al. 2008). Such findings suggest that the underlying process for increased TSPO in the early, inflammatory phase of MS may be different from that of the later chronic phase of MS.

The results of this [^{11}C]PBR28 PET study are consistent, in several respects, with results from the previous studies of TSPO using [^{11}C]PK11195. As was the case with [^{11}C]PBR28, among MRI-defined MS lesions, gadolinium-enhancing lesions showed the best correspondence with increased [^{11}C]PK11195 binding (Banati et al. 2000; Debruyne et al. 2003). There was poor correspondence (10–20%) between T_2 -hyperintense and T_1 -hypointense lesions and increased [^{11}C]PK11195 binding (Banati et al. 2000). Global TSPO expression either did not differ significantly between groups of healthy volunteers and subjects with MS (Debruyne et al. 2003), or only a minority demonstrated higher global TSPO expression in MS compared to healthy volunteers by [^{11}C]PK11195 PET (Banati et al. 2000).

The small sample size was a limitation of this study. The study was not controlled for the use of disease modifying therapies in subjects with MS which could potentially confound the analysis of the relationship between [^{11}C]PBR28 binding and measures of clinical disability. The study did, however, correct for differences in free plasma fraction of the radioligand. We have previously described low-affinity binding to [^{11}C]PBR28 in about 10% of the subjects we have studied to date, and excluded two subjects with MS for the current study due to low-affinity binding (Kreisl et al. 2010). In addition to low-affinity binders, Owen and colleagues recently identified another group of subjects that have mixed affinity—i.e., a mixture of high- and low-affinity binding to [^{11}C]PBR28 (Owen et al. 2010). While this is potentially a confounding factor, it would not affect the comparisons carried out in this study that are

within-subject or normalized. The strengths and the limitations of [^{11}C]PBR28 as a marker of TSPO in MS suggest that this radioligand could be utilized as a research tool to study the role of glial activation in the pathophysiology of MS. However, data is lacking at present with regard to the utility of [^{11}C]PBR28 as a biomarker in the clinical setting. Our results do not strongly support the role of [^{11}C]PBR28 as a predictive marker of disease progression in MS.

In summary, we report that [^{11}C]PBR28 PET shows altered distribution of brain TSPO expression in subjects with MS, characterized by increased ratio of white matter to gray matter fraction [^{11}C]PBR28 binding. Focal increase in [^{11}C]PBR28 binding corresponded to areas of active CNS inflammation as defined by gadolinium contrast enhancement on MRI, and in some cases preceded the appearance of MRI contrast enhancement, suggesting that glial activation may be an early event in MS lesion formation. Global [^{11}C]PBR28 binding levels were higher in subjects with longer disease duration in MS, and may reflect accumulation of TSPO in activated microglia and reactive astrocytes.

Acknowledgement We thank Maria Ferraris Araneta (MIB/NIMH) and Kaylan Fenton (NIB/NINDS) for clinical support. This research was supported by the Intramural Research Program of the NIH (NINDS and NIMH).

Conflict of interest The authors have no financial conflicts of interest to disclose.

References

- Bagasra O, Michaels FH, Zheng YM et al (1995) Activation of the inducible form of nitric oxide synthase in the brains of patients with multiple sclerosis. *Proc Natl Acad Sci USA* 92:12041–12045
- Banati RB, Newcombe J, Gunn RN et al (2000) The peripheral benzodiazepine binding site in the brain in multiple sclerosis: quantitative in vivo imaging of microglia as a measure of disease activity. *Brain* 123(Pt 11):2321–2337
- Briard E, Zoghbi SS, Imaizumi M et al (2008) Synthesis and evaluation in monkey of two sensitive ^{11}C -labeled aryloxyanilide ligands for imaging brain peripheral benzodiazepine receptors in vivo. *J Med Chem* 51:17–30
- Cosenza-Nashat M, Zhao ML, Suh HS et al (2008) Expression of the translocator protein of 18 kDa by microglia, macrophages and astrocytes based on immunohistochemical localization in abnormal human brain. *Neuropathol Appl Neurobiol* 35(3):306–328
- Debruyne JC, Versijpt J, Van Laere KJ et al (2003) PET visualization of microglia in multiple sclerosis patients using [^{11}C]PK11195. *Eur J Neurol* 10:257–264
- Fujita M, Imaizumi M, Zoghbi SS et al (2008) Kinetic analysis in healthy humans of a novel positron emission tomography radioligand to image the peripheral benzodiazepine receptor, a potential biomarker for inflammation. *Neuroimage* 40:43–52
- Henderson AP, Barnett MH, Parratt JD, Prineas JW (2009) Multiple sclerosis: distribution of inflammatory cells in newly forming lesions. *Ann Neurol* 66:739–753

- Katz D, Taubenberger JK, Cannella B, McFarlin DE, Raine CS, McFarland HF (1993) Correlation between magnetic resonance imaging findings and lesion development in chronic, active multiple sclerosis. *Ann Neurol* 34:661–669
- Kreisler WC, Fujita M, Fujimura Y et al (2010) Comparison of [(11)C]- (R)-PK 11195 and [(11)C]PBR28, two radioligands for translocator protein (18 kDa) in human and monkey: implications for positron emission tomographic imaging of this inflammation biomarker. *Neuroimage* 49:2924–2932
- Logan J (2003) A review of graphical methods for tracer studies and strategies to reduce bias. *Nucl Med Biol* 30:833–844
- Logan J, Fowler JS, Volkow ND et al (1990) Graphical analysis of reversible radioligand binding from time-activity measurements applied to [N-11C-methyl]-(-)-cocaine PET studies in human subjects. *J Cereb Blood Flow Metab* 10:740–747
- McDonald WI, Compston A, Edan G et al (2001) Recommended diagnostic criteria for multiple sclerosis: guidelines from the International Panel on the diagnosis of multiple sclerosis. *Ann Neurol* 50:121–127
- McEnery MW, Snowman AM, Trifiletti RR, Snyder SH (1992) Isolation of the mitochondrial benzodiazepine receptor: association with the voltage-dependent anion channel and the adenine nucleotide carrier. *Proc Natl Acad Sci USA* 89:3170–3174
- Owen DR, Howell OW, Tang SP et al (2010) Two binding sites for [(3)H]PBR28 in human brain: implications for TSPO PET imaging of neuroinflammation. *J Cereb Blood Flow Metab* 30:1608–1618
- Versijpt J, Debruyne JC, Van Laere KJ et al (2005) Microglial imaging with positron emission tomography and atrophy measurements with magnetic resonance imaging in multiple sclerosis: a correlative study. *Mult Scler* 11:127–134
- Werner P, Pitt D, Raine CS (2001) Multiple sclerosis: altered glutamate homeostasis in lesions correlates with oligodendrocyte and axonal damage. *Ann Neurol* 50:169–180
- Zhang Y, Brady M, Smith S (2001) Segmentation of brain MR images through a hidden Markov random field model and the expectation-maximization algorithm. *IEEE Trans Med Imaging* 20:45–57